Proceedings of the 28th IEEE
EMBS Annual International Conference
New York City, USA, Aug 30-Sept 3, 2006

Enhanced parameter estimation with GLLS and the Bootstrap Monte Carlo method for dynamic SPECT

Lingfeng Wen, *Member, IEEE* , Stefan Eberl, *Member, IEEE* , (David) Dagan Feng, *Fellow, IEEE*

***Abstract*—The generalized linear least squares (GLLS) method has been shown to successfully construct unbiased parametric images from dynamic positron emission tomography (PET). However, the high level of noise intrinsic in single photon emission computed tomography (SPECT) can give rise to unsuccessful voxel-wise fitting using GLLS, resulting in physiologically meaningless estimates, such as negative kinetic parameters for compartment models. In this study, three approaches were investigated to improve the reliability of GLLS applied to dynamic SPECT data. The simulation and experimental results showed that GLLS with the aid of Bootstrap Monte Carlo method proved successful in generating parametric images and preserving all of the major advantages of all the originally GLLS method, although at the expense of increased computation time.**

I. Introduction

Functional imaging, such as positron emission tomography (PET) and single photon emission computed tomography (SPECT), is capable of identifying subtle functional changes prior to anatomical changes being detectable by anatomical imaging. Parametric images, whose values represent quantitative parameters relevant to physiological or metabolic processes, require the fitting of an underlying kinetic model to voxel-wise tissue time activity curves (TTACs) for a given input function (IF) or reference region. The graphical methods such as the Patlak and Logan methods [1, 2], have been successfully applied for generating parametric images and are computational efficient and relatively insensitive to noise. However, they provide only a limited number of parameters (typically two) and frequently depend on some assumption about the underlying model, which may not be valid for a given tracer.

The GLLS method has been proposed as an unbiased, computationally efficient algorithm for kinetic parameter estimation without requiring a set of initial parameters to be specified [3]. Full kinetic parameters can be estimated by the GLLS method as well as being able to derive macro parameters such as the binding potential. The GLLS method has been successfully applied to PET data in the brain, heart and liver [3-5]. Recently, it has been applied to dynamic SPECT data for region of interest (ROI) derived tissue time activity curves (TTACs) [6]. However, the high level of noise intrinsic in SPECT can give rise to unsuccessful fits using GLLS, especially for voxel-wise TTACs, resulting in physiologically meaningless estimates, such as negative kinetic parameters for compartment models.

In this paper, three methods were investigated to enhance the reliability of GLLS. The first method was to incorporate a prior estimate of volume of distribution (V_d) in the fitting (V_d-aided GLLS). The second method was to apply Bootstrap Monte Carlo (BMC) method to generate multiple re-sampled TTACs for each voxel (BMC-aided GLLS). The third method was to combine the V_d-aided and BMC-aided GLLS together (BMC-V_d-aided GLLS). The performances of the proposed methods were evaluated by computer simulation and *in-vivo* studies.

II. Methods

A. V_d-aided GLLS

The volume of distribution (V_d) reflects the equilibrium distribution of the tracer in the tissue, which is relatively stable compared with other parameters. If V_d is known, the reliability of parameter estimates can be potentially improved due to reduced number of parameters in the estimation and constraints in the parametric domain.

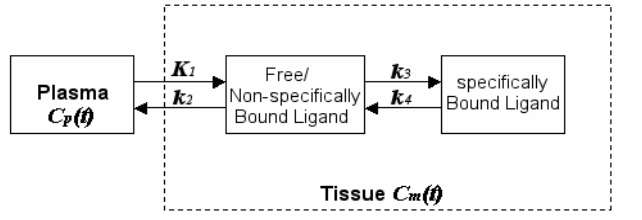

Fig.1 Three-compartment and four-parameter kinetic model for neuroreceptor study

For the 3-compartment and 4-parameter kinetic model as shown in Fig. l, the activity function in the tissue, $C_m(t)$, can be derived from the differential equations for the compartment model in (1), where $C_p(t)$ is the plasma time activity function.

Manuscript received March 29, 2006. This work was supported in part by the Australian Research Council (ARC) and University Grant Council of Hong Kong (UGC).

Lingfeng Wen is with School of Information Technologies, University of Sydney and Department of PET and Nuclear Medicine, Royal Prince Alfred Hospital (phone: +61-2-9515 6170; fax: +61-2-9351 3838; e-mail: wenlf@ ieee.org).

Stefan Eberl is with Department of PET and Nuclear Medicine, Royal Prince Alfred Hospital and School of Information Technologies, University of Sydney (e-mail: stefan@ it.usyd.edu.au).

(David) Dagan Feng is with School of Information Technologies, University of Sydney and Department of Electronic and Information Engineering, Hong Kong Polytechnic University (e-mail: feng@ it.usyd.edu.au).

$$\frac{d^2}{dt^2}C_m(t) = K_1\frac{d}{dt}C_p(t) + K_1(k_3+k_4)C_p(t) - (k_2+k_3+k_4)\frac{d}{dt}C_m(t) - k_2k_4C_m(t) \quad (1)$$

For the model in Fig.1, V_d is given by the definition in the following equation (2).

$$V_d = \frac{K_1}{k_2}(1+\frac{k_3}{k_4}) \quad (2)$$

Thus, the differential equation in (1) can be reorganized into (3),

$$\frac{d^2}{dt^2}C_m(t) = P_1\frac{d}{dt}C_p(t) + P_3\frac{d}{dt}C_m(t) + P_4[C_m(t) - V_dC_p(t)] \quad (3)$$

where, $P_1=K_1$, $P_3=-(k_2+k_3+k_4)$, $P_4=k_2k_4$. If the value of V_d is known or estimated a priori, the equation for parameter estimation of GLLS in [3] can be simplified to (4).

$$\theta_{Vd-GLLS} = (Z_{Vd}^T Z_{Vd})^{-1} Z_{Vd}^T \cdot r \quad (4)$$

where, $\theta_{Vd-GLLS} = [P_1, P_3, P_4]^T$,

$$\lambda_{1,2} = -\frac{\hat{P}_3 \pm \sqrt{\hat{P}_3 + 4\hat{P}_4}}{2}, \psi_1 = \frac{1}{\lambda_2-\lambda_1}(\lambda_2 e^{-\lambda_2 t} - \lambda_1 e^{-\lambda_1 t}),$$

$$\psi_2 = \frac{1}{\lambda_2-\lambda_1}(e^{-\lambda_1 t} - e^{-\lambda_2 t}),$$

$$Z_{Vd} = \begin{bmatrix} \psi_1 \otimes C_p(t_1), \psi_1 \otimes C_m(t_1), \psi_2 \otimes C_m(t_1) - V_d\psi_2 \otimes C_p(t_1) \\ \psi_1 \otimes C_p(t_2), \psi_1 \otimes C_m(t_2), \psi_2 \otimes C_m(t_2) - V_d\psi_2 \otimes C_p(t_2) \\ \vdots \\ \psi_1 \otimes C_p(t_n), \psi_1 \otimes C_m(t_n), \psi_2 \otimes C_m(t_n) - V_d\psi_2 \otimes C_p(t_n) \end{bmatrix},$$

$$r = \begin{bmatrix} C_m(t_1) + \hat{P}_3\psi_1 \otimes C_m(t_1) + \hat{P}_4\psi_2 \otimes C_m(t_1) \\ C_m(t_1) + \hat{P}_3\psi_1 \otimes C_m(t_2) + \hat{P}_4\psi_2 \otimes C_m(t_2) \\ \vdots \\ C_m(t_1) + \hat{P}_3\psi_1 \otimes C_m(t_m) + \hat{P}_4\psi_2 \otimes C_m(t_m) \end{bmatrix}.$$

For simplicity, the Logan method was used to derive the prior V_d estimates for V_d-aided GLLS.

B. BMC-aided GLLS and BMC-Vd-aided GLLS

The Bootstrap Monte Carlo (BMC) method is a resampling technique which allows multiple synthetic data sets to be derived from a measured data set [7]. Given a curve of *n* data points, *n* random samples are drawn with replacement to generate a new estimate of the true TTAC. Since replacement is used, some points are duplicated and others are not selected for a particular BMC sample and hence one does not simply get back the original curve each time. The BMC method has been shown to provide similar insight into parameter estimation reliability as the conventional Monte Carlo method [8].

Thus, BMC method was used to aid the curve fitting for both GLLS and Vd-aided GLLS. BMC curves were generated and fitted with GLLS. Results from BMC curves with unsuccessful fits, e.g. negative rate constants, were rejected. The mean of the estimated parameters from ten successful fits to BMC curves, derived for a particular voxel TTAC, were then used as the final parameter estimates for that voxel. For all the methods investigated, the values of voxels without successful fits were set to zero.

C. Computer Simulation and experimental data

High count Monte Carlo simulations were preformed to generate the noise-free projection data based on a mathematical human brain phantom. The dynamic projection data were then generated according to experimentally observed kinetics of the nicotinic receptor tracer 5-[^{123}I]-iodo-A-85380 [9]. Data sets with five different levels of Poisson noise, based on noise levels encountered experimentally, were generated. The projection data were reconstructed by the OS-EM iterative method with attenuation and scatter correction. The parametric images were derived by the studied methods.

The volumes of interests (VOI) derived from the phantom were used to generate the average parameters for thalamus, cerebellum and frontal cortex. 20 sets of dynamic data were simulated for each level of noise, to allow estimation of the percentage bias, as compared to the known reference value, and the coefficient of variation (CV) for the parameters of interests (the influx rate K_1 and volume of distribution V_d).

The studied methods were also used to generate the parametric images of K_1 and V_d from the experiments for the baboons' study on the nicotinic receptor [9].

III. Results

Fig.2 plots the percentage bias of parameter estimates K_1 and V_d for the frontal cortex from the simulations. Somewhat unexpectedly, the V_d-aided GLLS suffered from the most bias for both K_1 and V_d and higher bias than that observed by the original GLLS method. Thus the incorporation of prior V_d estimates did not improve the GLLS method for noisy SPECT data. Both the BMC-aided and BMC-V_d-aided GLLS methods substantially reduced the bias by avoiding unsuccessful fits, which would have resulted in the corresponding voxel values to be set to zero.

Fig.3 plots the CV of parameter estimates K_1 and V_d for the frontal cortex from the simulations. The CV for most methods was low and generally <2.5%, with the exception of the CV of V_d estimated by the original GLLS, which reached nearly 8%.

Similar results were also observed in the thalamus and cerebellum except that the BMC-aided GLLS overestimated V_d. As no corrections for partial volume effects were applied, an underestimation i.e. negative bias is expected due to marked partial volume effects. The overestimation of V_d by the BMC-aided GLLS demonstrates one of the potential limitations of this method. As only successful fits are retained from the up to 200 BMC generated curves per voxel, it appears that at least for these data, success in fitting with GLLS is biased towards resampled curves which tend

towards higher V_d values. It was also in line with expectation that the integration of prior information of V_d could improve the estimated accuracy with the Bootstrap MC method. The simulation results demonstrated that the V_d-aided GLLS still suffered from unsuccessful fitting, despite reducing the number of parameters which have to be estimated.

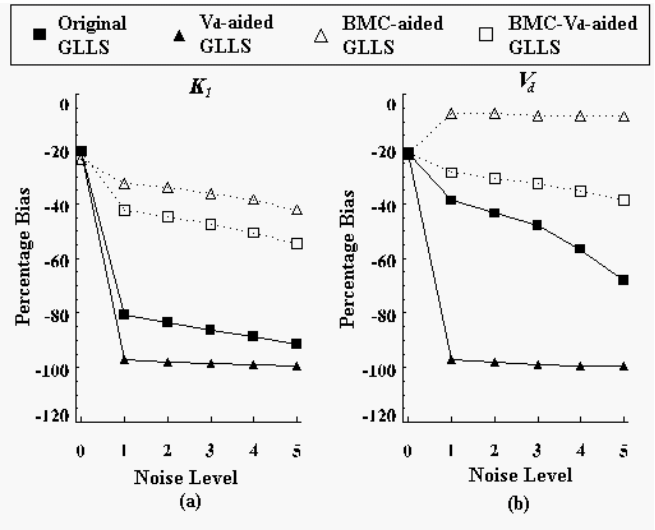

Fig.2 Percentage bias as a function of increasing noise level for the frontal cortex. (a) percentage bias of K_1 (b) percentage bias of V_d

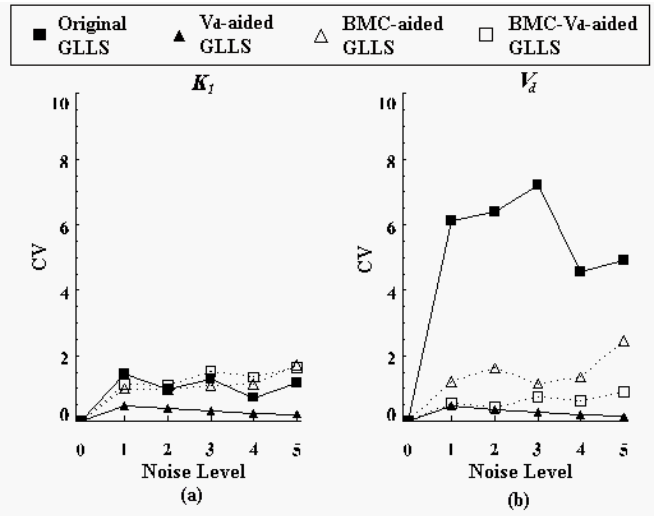

Fig.3 CV as a function of increasing noise level for the frontal cortex. (a) CV of K_1 (b) CV of V_d

Compared to the original GLLS computation time, the average running time were 1.0, 61.7 and 83.2 times higher for the V_d-aided, BMC-aided, BMC-V_d-aided GLLS, respectively.

Fig.4 and Fig.5 show the parametric images of K_1 and V_d derived by the studied methods for experimental data. Although the Vd-aided GLLS seems to remove 'outliers' compared with the original GLLS, it suffered from a large number of unsuccessful fits. For BMC-aided and BMC-V_d-aided GLLS, no marked differences were observed for K_1 between the two methods, while the BMC-V_d-aided GLLS achieved better parametric images for V_d.

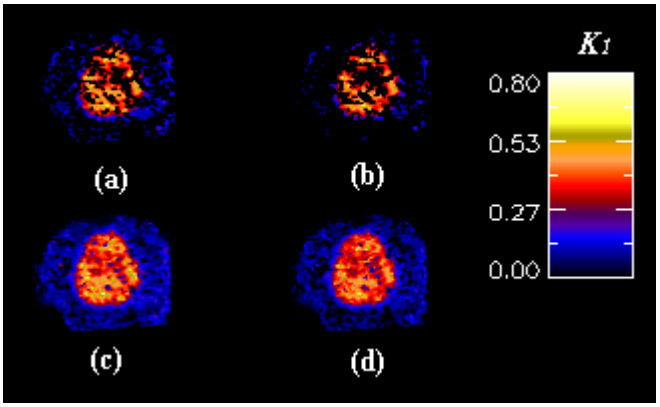

Fig.4 Parametric images of K_1 for the experimental data derived by (a) original GLLS, (b) V_d-aided GLLS, (c) BMC-aided GLLS and (d) BMC-V_d-aided GLLS.

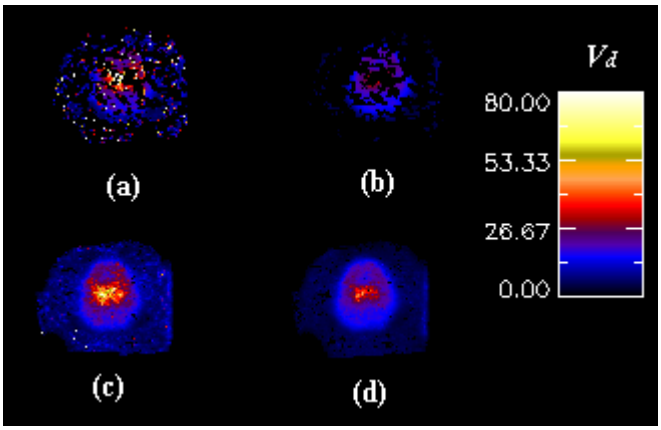

Fig.5 Parametric images of V_d for the experimental data derived by (a) original GLLS, (b) V_d-aided GLLS, (c) BMC-aided GLLS and (d) BMC-V_d-aided GLLS.

IV. Conclusion

Three methods were investigated to enhance the GLLS method to deal with the noisy SPECT data. The results showed that the V_d-aided GLLS couldn't improve the reliability of estimating parametric images, while the BMC-aided and BMC-V_d-aided GLLS proved successful in generating parametric images at the expense of increased computation time. The BMC-aided GLLS provided less biased estimates of K_1 and the BMC-V_d-aided GLLS method provided less bias and more reliable estimates of V_d.

References

[1] C. S. Patlak, R. G. Blasberg, and J. D. Fenstermacher, "Graphical evaluation of blood-to-brain transfer constants from multiple-time uptake data," J. Cereb. Blood Flow Metab., vol. 3, pp. 1-7, 1983.

[2] J. Logan, J. S. Fowler, N. D. Volkow, et al., "Graphical analysis of reversible radioligand binding from time-activity measurements applied to [N-11C-methyl]-(-)-cocaine PET studies in human subjects," J. Cereb. Blood Flow Metab., vol. 10, pp. 740-747, 1990.

[3] D. Feng, S. C. Huang, Z. Wang, et al., "An unbiased parametric imaging algorithm for nonuniformly sampled biomedical system parameter estimation," IEEE Trans. Med. Imaging, vol. 15, pp. 512-518, 1996.

[4] K. Chen, M. Lawson, E. Reiman, et al., "Generalized linear least squares method for fast generation of myocardial blood flow parametric images with N-13 Ammonia PET," IEEE Trans. Med. Imaging, vol. 17, pp. 236-243, 1998.
[5] H. C. Choi, S. Chen, D. Feng, et al., "Fast parametric imaging algorithm for dual-input biomedical system parameter estimation," Comput. Meth. Programs Biomed. Accepted.
[6] L. Wen, S. Eberl, W. Cai, et al., "A Reliable Voxexl-by-Voxel Parameter Estimation for Dynamic SPECT," presented at World Congress on Medical Physics and Biomedical Engineering, Sydney, Australia, 2003.
[7] W. H. Press, S. A. Teukolsky, W. T. Vetterling, et al., "Confidence Limits on Estimated Model Parameters," in Numerical Recipes in C: The art of scientific computing, 2 ed. Cambridge: Cambridge University Press, 1992, pp. 689-699.
[8] L. Wen, S. Eberl, K. P. Wong, et al., "Effect of reconstruction and filtering on kinetic parameter estimation bias and reliability for dynamic SPECT: A simulation study," IEEE Trans. Nucl. Sci., vol. 52, no.1, pp. 69-78, Feb 2005.
[9] M. Kassiou, S. Eberl, S. R. Meikle, et al., "In vivo imaging of nicotinic receptor upregulation following chronic (-)-nicotine treatment in baboon using SPECT," Nucl. Med. Biol., vol. 28, pp. 165-175, 2001.